

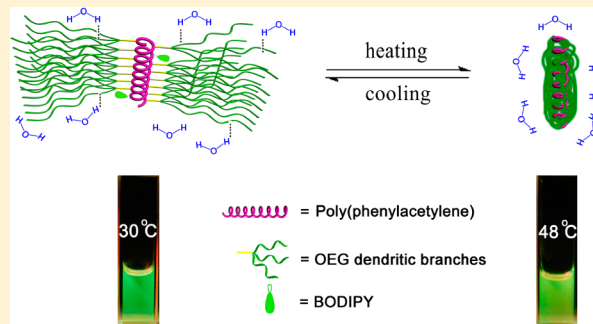
Thermoresponsive Helical Poly(phenylacetylene)s

Shu Li, Kun Liu, Guichao Kuang,* Toshio Masuda, and Afang Zhang*

Laboratory of Polymer Chemistry, Department of Polymer Materials, College of Materials Science and Engineering, Shanghai University, Nanchen Street 333, Materials Building Room 447, Shanghai 200444, China

Supporting Information

ABSTRACT: Poly(phenylacetylene) (PPA) bearing dendritic oligo(ethylene glycol) (OEG) as pendants was synthesized, and its thermoresponsiveness and helical conformation were investigated. Despite the steric hindrance of the bulky pendants in the homopolymer PPA-OEG, the chirality could be efficiently transferred from pendant alanine moieties to PPA main chain through ester linkage. In order to examine the steric effect of pendants on chiral transformation, a model PPA homopolymer PPA-Boc which carries less bulky moieties was prepared for comparison. The chiroptical properties of these thermoresponsive PPAs were further investigated by varying temperature to examine the effects of their thermoresponsiveness. In addition, PPA copolymers PPA-BDY bearing OEG dendron and fluorescent boradiazaindacene (BDY) chromophore showed excellent thermoresponsive properties and interesting fluorescence enhancement at elevated temperatures. To investigate the rigidity effects of polymer backbone on the thermally induced fluorescence enhancement, a nonchiral polymer carrying the same pendants but with polymethacrylate as the backbone (PMA-OEG) was prepared. It was found that the chiroptical and fluorescence properties of these PPAs are dependent not only on their chemical structures but also on the thermoresponsiveness.



INTRODUCTION

The increased understanding of the π -conjugated polymers has stimulated advances in cross-disciplinary areas of materials sciences, biological chemistry, and biomedical therapy.¹ As a class of widely studied π -conjugated polymers, poly(phenylacetylene) (PPA) and its derivatives exhibit interesting properties such as liquid crystallinity, electrical conductivity, catalysis, fluorescence sensing, and chiral recognition.² One intriguing property for PPAs is that they can be mediated to adopt helical conformation with preferred handedness, which have attracted great interest in the past decades.³ In principle, PPA derivatives adopt a dynamic conformation whose helical sense is governed by hydrogen bonds between pendant amide groups or by steric hindrance from bulky substituents.⁴ Various helical PPAs have been reported, and chirality transmission from pendant chiral groups to the polymer main chain can be significantly amplified through covalent bonds⁵ or by non-covalent interactions.⁶ The magnitude of Cotton effects from circular dichroism (CD) spectra depends greatly on the distance between chiral center and the backbone.^{3b} Although PPAs display increased molar ellipticity with increasing substituent bulkiness, most dendronized PPAs show decreased CD intensity with increase of dendritic generations due to the overcrowded pendants. It has been documented that the handedness and compactness of helical PPAs depend on the chirality of the pendants,^{3–6} metal coordination,⁷ polar or donor effects of solvents,⁸ and temperature.^{8d,e,9}

Combination of stimuli responsiveness with conjugated polymers will not only afford these polymers novel

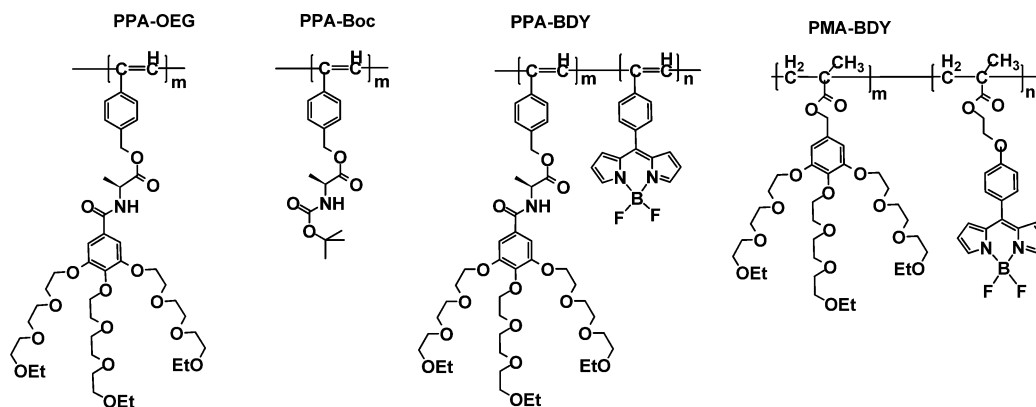
functionalities but also pave a new avenue to broaden their applications; thus, helical polymers capable of responding to external stimuli have received considerable attention. For example, functional PPAs which are responsive to chirality were proposed by Yashima to tune the preferential helical conformation and to switch the helical sense through host–guest^{6,10} or acid–base interactions.¹¹ PPAs bearing riboflavin pendants were found to show switchable helicity triggered by reduction–oxidation.¹² PPAs carrying azobenzene pendants were reported by Tang to show photoinduced isomerization.¹³ PPAs bearing urea acceptors are responsive to anions and, therefore, can be used for colorimetric detection of anions depending on their sizes. The PPAs display different colors related to the compactness of their helical conformation, which was utilized successfully by Kakuchi to identify different anions in organic¹⁴ or aqueous solutions.¹⁵ PPAs carrying free amino groups were found by Hu to be responsive to benzoic acid, and their helical conformation can be mediated accordingly.¹⁶ Recently, attention has been paid to thermoresponsive helical polymers because temperature is one of the most convenient parameters to change. Attaching oligoethylene glycol (OEG) pendants to helical polymers, we demonstrated that chiral polyisocyanides can be afforded thermoresponsiveness with tunable cloud point temperatures (T_{cp}).¹⁷ Thermoresponsive polyisocyanides carrying OEGs were also reported by Nolte

Received: February 18, 2014

Revised: April 11, 2014

Published: May 5, 2014

Chart 1. Chemical Structures of the Polymers Discussed in the Present Study



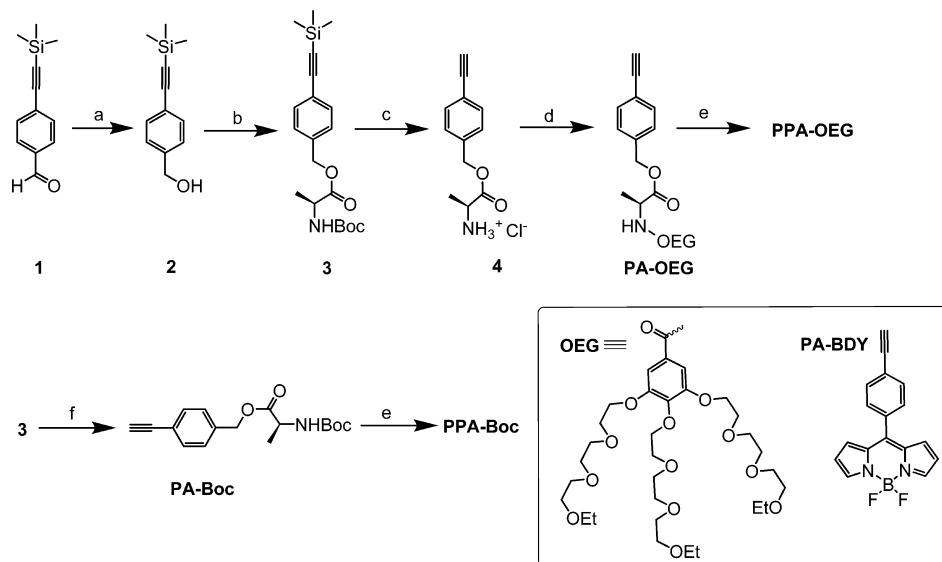
and found to form thermally induced hydrogels.¹⁸ Attaching OEG moieties of different chain lengths to polyisocyanates (PICs), Kakuchi reported that functional PICs can be thermoresponsive with T_{cp} dependent on their molar masses.¹⁹

We initiated a research program recently to address the versatile thermoresponsive polymers with three-folded OEG-based dendrons through covalent linkage²⁰ or supramolecular interaction²¹ and found that these polymers showed fast and sharp phase transitions without obvious hysteresis. In implementing our previous studies about thermoresponsive dendronized polymers, a series of thermoresponsive helical polyisocyanides carrying dipeptide pendants and OEG terminals were prepared.¹⁷ T_{cp} s of these polymers are not only dependent on their overall hydrophilicity and molar masses but also predominately related to their ordered secondary structures. Considering the high rigidity of polyisocyanides, it was found that the thermally induced aggregation did not show an obvious influence on the helical conformation. Inspired by this progress on the helical and thermoresponsive dendronized polymers, we here report on the first example of thermoresponsive PPAs. These polymers carry the first-generation three-folded dendritic OEG units through alanine linkage (Chart 1). They were synthesized through macromonomer route with a rhodium(I) catalyst and characterized with NMR spectroscopy and atomic force microscopy (AFM). CD measurements were performed to investigate chirality transformation from stereogenic center of pendants to the polymer main chain through an ester linkage. In order to compare the possible steric hindrance aroused from the bulky dendron in biasing helical sense of the polymers, model polymer PPA-Boc bearing a much smaller pendant Boc-protected alanine was prepared. The thermoresponsiveness of these chiral PPAs was investigated by turbidity measurements with UV/vis spectroscopy. In view of promising applications of these thermoresponsive PPAs as fluorescent thermometer, thermoresponsive helical copolymer PPA-BDY, which contains a small amount of boradiazaindacene (BDY) chromophore, was prepared, and its fluorescence properties during thermally induced phase transition processes were followed with UV/vis and fluorescence spectroscopies. In order to compare the effects of polymer backbone rigidity and helicity on thermally induced fluorescence properties, a much more flexible and achiral copolymer PMA-BDY, which contains a polymethacrylate backbone and a small amount of BDY chromophores as pendants, was synthesized.

EXPERIMENTAL SECTION

Materials. Compound OEG-OH was prepared according to our previous report.^{21a} Azobis(isobutyronitrile) (AIBN) was recrystallized twice from methanol. Dichloromethane (DCM) was dried over CaH_2 . Tetrahydrofuran (THF) was predried over sodium and refluxed over LiAlH_4 before use. Triethylamine (TEA) was dried over sodium hydroxide (NaOH) pellets. Other reagents and solvents were purchased at reagent grade and used without further purification. All synthetic steps for monomer synthesis were run under a nitrogen atmosphere. Macherey-Nagel precoated TLC plates (silica gel 60 G/UV254, 0.25 mm) were used for thin-layer chromatography (TLC) analysis. Silica gel 60 M (Macherey-Nagel, 0.040–0.063 mm, 200–300 mesh) was used as the stationary phase for column chromatography. All samples were kept under high vacuum prior to analytical measurements to remove strongly adhering solvent molecules.

Instrumentation and Measurements. ^1H and ^{13}C NMR spectra were recorded on a Bruker AV 500 (^1H : 500 MHz; ^{13}C : 125 MHz) spectrometer, and chemical shifts are reported as δ (ppm) relative to internal tetramethylsilane. High-resolution MALDI-TOF-MS analyses were performed on Ionspec Ultra instruments. Gel permeation chromatography (GPC) measurements were carried out on a Waters GPC e2695 instrument with a three-column set (Styragel HR3 + HR4 + HR5) equipped with refractive index detector (Waters 2414) and DMF (containing 1 g L^{-1} LiBr) as eluent at 45°C . Multiangle light scattering detector (Wyatt Technology Corporation, Down EOS 243-E) was used for some of the measurements. The calibration was performed with poly(methyl methacrylate) standards (from Polymer Standards Service-USA Inc.) with molar masses (M_p) in the range of 2580–981 000. Light scattering (LS) measurements were performed on an ALV/CGS-3 compact goniometer system with an ALV/LSE-5004 correlator and a Uniphase HeNe laser (22 mW output power at $\lambda = 632.8 \text{ nm}$ wavelength). CD measurements were performed on a JASCO J-815 spectropolarimeter with a thermo-controlled 1 mm quartz cell (three accumulations, “continue scanning” mode, scanning speed: 100 nm min^{-1} ; data pitch: 0.5 nm; response: 1 s; bandwidth: 2.0 nm). UV/vis turbidity measurements were carried out on a PE UV/vis spectrophotometer (Lambda 35) equipped with a thermo-controlled bath. Aqueous polymer solutions were placed in the spectrophotometer (path length 1 cm) and heated or cooled at a rate of 0.2 K min^{-1} . The absorptions of the solutions at $\lambda = 600 \text{ nm}$ were recorded per 5 s. The cloud point temperature (T_{cp}) was determined as the one at which the transmittance at $\lambda = 600 \text{ nm}$ reached 50% of its initial value. AFM measurements were performed on a Bruker Nanoscope VIII Multi-Mode microscope with an “E” scanner (scanning range $10 \mu\text{m} \times 10 \mu\text{m}$) and operated in peak force mode at room temperature in air. Bruker silicon tip was attached on nitride lever cantilevers (T : $0.65 \mu\text{m}$; L : $115 \mu\text{m}$; W : $25 \mu\text{m}$; f_0 : $70 \mu\text{m}$; k : 0.4 N/m). Samples were prepared from chloroform solutions by spin-coating with a speed of 2000 rpm. The scanning rate was at line frequency of 1.0 Hz. The images analyses were performed by using Nanoscope image processing software. The fluorescence spectra were

Scheme 1. Synthetic Procedures for the Monomers and Polymers^a

^aReagents and conditions: (a) **1**, LiAlH₄, THF, 0 °C, 4 h (83%); (b) **2**, L-Boc-Ala-OH, EDC·HCl, DMAP, DCM, 0 °C–rt, 29 h (89%); (c) **3**, HCl, ethyl acetate, 0 °C–rt, 8.5 h (98%); (d) **4**, OEG-OH, EDC·HCl, HOBt, DCM, 0 °C–rt, 22 h (58%); (e) PA-OEG, PA-BDY or PA-Boc, [(nbd)RhCl]₂, TEA, THF, 25 °C, 22 h for PPA-OEG (43%); 17 h for PPA-BDY (60%); 19 h for PPA-Boc (80%). (f) **3**, TBAF, CH₃OH, rt, 24 h for PA-BDY (79%), 16 h for PA-Boc (80%). Abbreviations: DCM = dichloromethane, DMAP = 4-(dimethylamino)pyridine, EDC·HCl = 1-(3-dimethylaminopropyl)-3-ethylcarbodiimide hydrochloride, HOBt = 1-hydroxy-1H-benzotriazole, TBAF = tetrabutylammonium fluoride, THF = tetrahydrofuran, [(nbd)RhCl]₂ = bicyclo[2.2.1]hepta-2,5-diene–rhodium(I) chloride dimer.

recorded on a spectrophotometer (Horiba Jobin Yvon Fluorolog-3) equipped with a Peltier temperature controller and heated or cooled at a rate of 0.2 K min⁻¹.

Synthesis of Monomer and Polymers. Compound 2. Compound **1** (1.00 g, 4.90 mmol) in THF (60 mL) was added dropwise to the THF solution (10 mL) of LiAlH₄ (0.37 g, 9.80 mmol) at 0 °C. The reaction mixture was stirred for another 4 h. Then, H₂O was added dropwise at 0 °C until no bubble was observed. The generated precipitate was dissolved by adding hydrochloric acid solution (5 mL, 10 wt %). After evaporation of THF, the residue was dissolved with DCM and washed with brine. The organic phase was dried over MgSO₄. Purification by chromatography using DCM as eluent afforded compound **2** as white solids (0.83 g, 83%). ¹H NMR (CDCl₃): δ = 0.25 (s, 9H, CH₃), 1.82 (br, 1H, OH), 4.68 (d, J = 4.1 Hz, 2H, CH₂), 7.28 (d, J = 7.9 Hz, 2H, Ar–H), 7.46 (d, J = 7.9 Hz, 2H, Ar–H).

Compound 3. Compound **2** (0.50 g, 2.45 mmol) in DCM (2 mL) was added to a DCM solution (20 mL) of L-Boc-Ala-OH (0.56 g, 2.90 mmol) and DMAP (0.15 g, 0.49 mmol). EDC·HCl (0.70 g, 3.68 mmol) was added slowly to the solution at 0 °C. The mixture was stirred at room temperature for 29 h before partitioned between brine and DCM. The organic phase was dried over MgSO₄. After filtration, the solvent was evaporated *in vacuo*. The residue was purified with a chromatograph using DCM/MeOH (50:1) as eluent to afford compound **3** as white solids (0.82 g, 89%). ¹H NMR (CDCl₃): δ = 0.25 (s, 9H, CH₃), 1.39 (d, J = 7.2 Hz, 3H, CH₃), 1.43 (s, 9H, CH₃), 4.34–4.36 (m, J = 7.1 Hz, 1H, CH), 5.16 (dd, J = 12.8, 36.6 Hz, 2H, CH₂), 7.27 (d, J = 8.0 Hz, 2H, Ar–H), 7.45 (d, J = 8.2 Hz, 2H, Ar–H).

Compound 4. Ethyl acetate solution of HCl (4.02 g, 110 mmol) was added dropwise to the ethyl acetate solution (10 mL) of compound **3** (0.96 g, 2.57 mmol) at 0 °C. The mixture was stirred at room temperature for 6 h. Evaporation of the solvent afforded compound **4** as white solids (0.80 g, 98%). ¹H NMR (D₂O): δ = 1.54 (d, J = 7.3 Hz, 3H, CH₃), 3.52 (s, 1H, CH), 4.21 (dd, J = 7.4, 14.6 Hz, 1H, CH), 5.28 (dd, J = 12.4, 17.7 Hz, 2H, CH₂), 7.42 (d, J = 8.1 Hz, 2H, Ar–H), 7.57 (d, J = 8.2 Hz, 2H, Ar–H).

Monomer PA-OEG. DCM solution (5 mL) of compound **4** (0.20 g, 0.52 mmol) and DIPEA (0.13 g, 1.00 mmol) was added to the DCM

solution (10 mL) of OEG-OH (0.34 g, 0.52 mmol) and 1-hydroxy-1H-benzotriazole (HOBt; 0.09 g, 0.65 mmol). EDC·HCl (0.12 g, 0.60 mmol) was added slowly to the mixture solution at 0 °C. The mixture solution was stirred at room temperature for 24 h before partitioned between brine and DCM. The organic phase was dried over MgSO₄. After filtration, the solvent was evaporated *in vacuo*. The residue was purified with chromatograph by using DCM/MeOH (60:1) as eluent to afford monomer PA-OEG as white solids (0.25 g, 58%). ¹H NMR (CDCl₃): δ = 1.16–1.20 (m, 9H, CH₃), 1.51 (d, J = 7.1 Hz, 3H, CH₃), 3.10 (s, 1H, CH), 3.48–3.84 (m, 38H, CH₂), 4.18–4.21 (m, 6H, CH₂), 4.76–4.79 (m, 1H, CH), 5.18 (dd, J = 12.6, 25.8 Hz, 2H, CH₂), 6.75 (d, J = 7.2 Hz, NH), 7.09 (s, 2H, Ar–H), 7.30 (d, J = 8.2 Hz, 2H, Ar–H), 7.46 (d, J = 8.2 Hz, 2H, Ar–H). ¹³C NMR (CDCl₃): δ = 14.96, 18.02, 26.56, 31.31, 36.51, 48.49, 66.29, 68.95, 69.60, 70.51, 72.24, 77.80, 82.88, 107.27, 127.73, 128.45, 128.69, 132.08, 135.93, 152.21, 162.38, 166.33, 172.66. HRMS (ESI): *m/z* calcd for C₄₃H₆₅NO₁₅ [M + Na]⁺: 858.4266, found: 858.4246.

Monomer PA-Boc. Tetrabutylammonium fluoride (TBAF) (0.54 g, 1.70 mmol) was added to the methanol solution of compound **3** (0.20 g, 0.53 mmol) at room temperature. After being stirred for 16 h, methanol was evaporated. The residue was partitioned between brine and DCM. The organic phase was dried over MgSO₄. After filtration, the solvent was evaporated *in vacuo*. The residue was purified with chromatograph using hexane/EtOAc (5:1) as eluent to afford monomer PA-Boc as a white oil (0.12 g, 80%). ¹H NMR (CDCl₃): δ = 1.38 (d, J = 7.2 Hz, 3H, CH₃), 1.43 (s, 9H, CH₃), 3.09 (s, 1H, CCH), 4.34–4.37 (m, 1H, CH), 5.02 (br, 1H, NH), 5.07–5.19 (m, 2H, CH₂), 7.29 (d, J = 8.1 Hz, 2H, Ar–H), 7.47–7.49 (d, J = 8.2 Hz, 2H, Ar–H).

Monomer PA-BDY was prepared according to previous report²² with a yield of 80%. ¹H NMR (CDCl₃): δ = 3.26 (s, 1H, CCH), 6.56 (d, J = 3.8 Hz, 2H, pyrrole-H), 6.91 (d, J = 4.1 Hz, 2H, pyrrole-H), 7.54 (d, J = 8.4 Hz, 2H, Ar–H), 7.65 (d, J = 8.2 Hz, 2H, Ar–H), 7.95 (s, 2H, pyrrole-H). ¹³C NMR (CDCl₃): δ = 80.09, 82.61, 118.86, 124.94, 130.50, 131.48, 132.20, 134.07, 134.75, 144.55, 146.22. HRMS (ESI): *m/z* calcd for C₁₇H₁₁BF₂N₂ [M + H]⁺: 291.1021, found: 291.1042.

Polymer PPA-OEG. THF solution (0.5 mL) of [(nbd)RhCl]₂ (1.1 mg, 0.002 mmol) and TEA (2 mg, 0.02 mmol) were added to the

Table 1. Polymerization Conditions and Characterization Results of the Polymers

entries	polymerization conditions					yield (%)	[BDY] ^a (mol %)	GPC results ^b			
	[M]/[I]	[M] (mol/L)	time (h)	solvent	temp (°C)			M _w (×10 ⁻⁴)	DP	PDI	T _{cp} ^c (°C)
PPA-OEG	50:1	0.096	22	THF	25	42	0	67.5	311	2.59	36.0
PPA-BDY	50:1	0.096	17	THF	25	60	1/957	49.4	307	1.93	36.2
PMA-BDY	23:1	2.80	25	DMF	70	55	1/1018	30.1	175	2.39	35.0
PPA-Boc	50:1	0.096	19	THF	25	67	0	34.2	369	3.03	NA

^aDetermined by comparison of the absorbance ($A_{500\text{ nm}}$) for PPA-BDY with PA-BDY ($\epsilon_{500\text{ nm}} = 63\,700\text{ M}^{-1}\text{ cm}^{-1}$) in methanol or the absorbance ($A_{498\text{ nm}}$) for PMA-BDY with MA-BDY ($\epsilon_{498\text{ nm}} = 81\,300\text{ M}^{-1}\text{ cm}^{-1}$) in DCM at 25 °C, respectively (Figure S3 in Supporting Information).

^bDetermined by GPC with DMF as eluent. ^cThe apparent T_{cp} of the polymers was determined as the temperature at 50% of the initial transmittance at $\lambda = 600\text{ nm}$. NA = not available.

THF solution (0.5 mL) of PA-OEG (80 mg, 0.096 mmol). The mixture was stirred at 25 °C for 22 h before concentrated on a rotary evaporator. The residue was purified with chromatograph by using DCM as eluent to afford polymer PPA-OEG as yellow solids (34 mg, 43%). ¹H NMR (CDCl₃, 50 °C): $\delta = 1.11\text{--}1.18$ (m, 9H, CH₃), 1.24–1.37 (br, 3H, CH₃), 3.41–3.73 (m, 37H, CH₂ + CH₂), 4.05 (d, $J = 31.8\text{ Hz}$, 6H, CH₂), 4.65 (br, 1H, CH), 4.83 (br, 1H, CH₂), 4.95 (br, 1H, CH₂), 5.61 (br, 1H, CCH), 6.62 (br, 2H, Ar–H), 6.93 (br, 2H, Ar–H), 7.05 (br, 2H, Ar–H), 7.72 (br, H, NH).

Polymer PPA-BDY. THF stock solution (0.5 mL) of PA-BDY (0.10 mg, 0.34 mol), [(nbd)RhCl]₂ (1.1 mg, 0.002 mmol), and TEA (2.0 mg, 0.02 mmol) were added to the stock solution (0.5 mL) of PA-OEG (150 mg, 0.18 mmol). The mixture solution was stirred at 25 °C for 17 h before concentrated on a rotary evaporator. The residue was purified with a chromatograph by using DCM as eluent to afford polymer PPA-BDY as yellow solids (90 mg, 60%). ¹H NMR (CDCl₃, 50 °C): $\delta = 1.11\text{--}1.18$ (m, 9H, CH₃), 1.24–1.37 (br, 3H, CH₃), 3.41–3.73 (m, 37H, CH₂ + CH₂), 4.05 (d, $J = 31.8\text{ Hz}$, 6H, CH₂), 4.65 (br, 1H, CH), 4.83 (br, 1H, CH₂), 4.95 (br, 1H, CH₂), 5.61 (br, 1H, CCH), 6.63 (br, 2H, Ar–H), 6.94 (br, 2H, Ar–H), 7.06 (br, 2H, Ar–H), 7.80 (br, H, NH).

Polymer PPA-Boc. THF solution (0.5 mL) of [(nbd)RhCl]₂ (1.1 mg, 0.002 mmol) and TEA (2.0 mg, 0.020 mmol) were added to the THF solution (0.5 mL) of PA-Boc (100 mg, 0.33 mmol). The mixture solution was stirred at 25 °C for 19 h before concentrated on a rotary evaporator. The residue was purified with chromatograph by using DCM as eluent to afford polymer PPA-Boc as yellow solids (80 mg, 80%). ¹H NMR (DMSO-*d*₆, 80 °C): $\delta = 1.19$ (d, $J = 7.2\text{ Hz}$, 3H, CH₃), 1.33 (s, 9H, CH₃), 4.02–4.05 (m, 1H, CH), 4.87 (dd, $J = 12.8, 34.6\text{ Hz}$, 2H, CH₂), 5.70 (s, 1H, CCH), 6.60 (d, $J = 6.7\text{ Hz}$, 2H, Ar–H), 6.94 (d, $J = 7.5\text{ Hz}$, 2H, Ar–H).

RESULTS AND DISCUSSION

Synthesis and Structural Characterization of Homo- and Copolymers. The synthesis of phenylacetylene monomers PA-OEG and PA-Boc started from the same commercially available aldehyde **1** as depicted in Scheme 1. Reduction of **1** with LiAlH₄ gave corresponding alcohol **2**, which was treated with *N*-(*tert*-butoxycarbonyl)-L-alanine (L-Boc-Ala-OH) to give compound **3** with protected alkyne and amine. Monodeprotection of trimethylsilyl (TMS) group with TBAF provided monomer PA-Boc. Double deprotection of both TMS and Boc groups with HCl yielded **4**. Its amidation with OEG-OH yielded monomer PA-OEG by applying a typical peptide coupling method in the presence of EDC and HOBT. The monomer PA-BDY was prepared according to the literature.²² The synthesis of aliphatic monomer MA-BDY was similar to that for PA-BDY with the exception of final methacrylation reaction (refer to Scheme S1 in the Supporting Information). All new compounds were identified by ¹H NMR spectroscopy, and new monomers were further characterized by ¹³C NMR spectroscopy as well as high-resolution mass spectrometry.

The polymerizations of phenylacetylene monomers were carried out by using [(nbd)RhCl]₂ catalyst with a constant monomer/catalyst ratio of 50/1 in polar solvent THF at 25 °C. TEA was added as a base, which could greatly accelerate the reaction and facilitate to obtain high molecular weight polymers.²³ All polymerizations proceeded homogeneously without obvious viscosity changes. A typical free radical copolymerization was conducted for the methacrylate monomers by using AIBN as initiator (see Supporting Information for details). All polymers are totally soluble in common organic solvents or in water. They were purified through silica-gel column chromatography with DCM as eluent, and the total monomer conversions were calculated gravimetrically. The molar masses of obtained polymers measured by GPC with DMF as eluent were in the range of millions g·mol⁻¹. Detailed polymerization conditions and characterization results for the polymers/copolymers are summarized in Table 1. The weight-average molecular weights (M_w) of PPA-OEG and PPA-BDY determined by GPC analyses are 6.75×10^5 and 4.94×10^5 , respectively. However, the corresponding M_w s were determined by static laser scattering to be 3.01×10^6 and 2.30×10^6 , respectively, indicating that GPC measurements underestimate significantly the molar masses of these polymers comprising repeat units of high molar mass.¹⁷

All polymer structures were characterized by ¹H NMR spectroscopy (for spectra, see Supporting Information). As an example, the ¹H NMR spectra of monomer PA-OEG and its corresponding homopolymer PPA-OEG, together with the model polymer PPA-Boc, are combined in Figure 1. The proton signal at $\delta = 3.09\text{ ppm}$ ascribed to the proton of ethynyl group from the monomer PA-OEG disappeared for polymer PPA-OEG; instead, a new peak at $\delta = 5.68\text{ ppm}$ appeared which is ascribed to the olefinic proton from the conjugated main chain.²⁴ Besides, the proton signals from PPA-OEG broadened when compared to these from the corresponding monomer. These results strongly demonstrate successful transformation from monomer PA-OEG to polymer PPA-OEG. Highly stereoregular *cis*-transoidal conformation for the PPA main chain is expected since a rhodium catalyst was used.²⁵ According to the calculation methods proposed by Percec and co-workers,²⁶ the *cis*-content was determined to be 92% for PPA-OEG. In contrast to the sharp and well-resolved proton signals from PPA-Boc, the broadened proton signals from PPA-OEG (Figure 1) indicate that the polymer is more rigid than PPA-Boc in CDCl₃ solution. Attention was paid to the splitting of the proton signals (*f*) of methyl group from alanine moiety in the monomer and polymers. Both the monomer PA-OEG and the model polymer PPA-Boc showed the expected symmetric doublet. The chemical shift difference between the split peaks ($\Delta\delta$) was about 0.014 ppm. While for

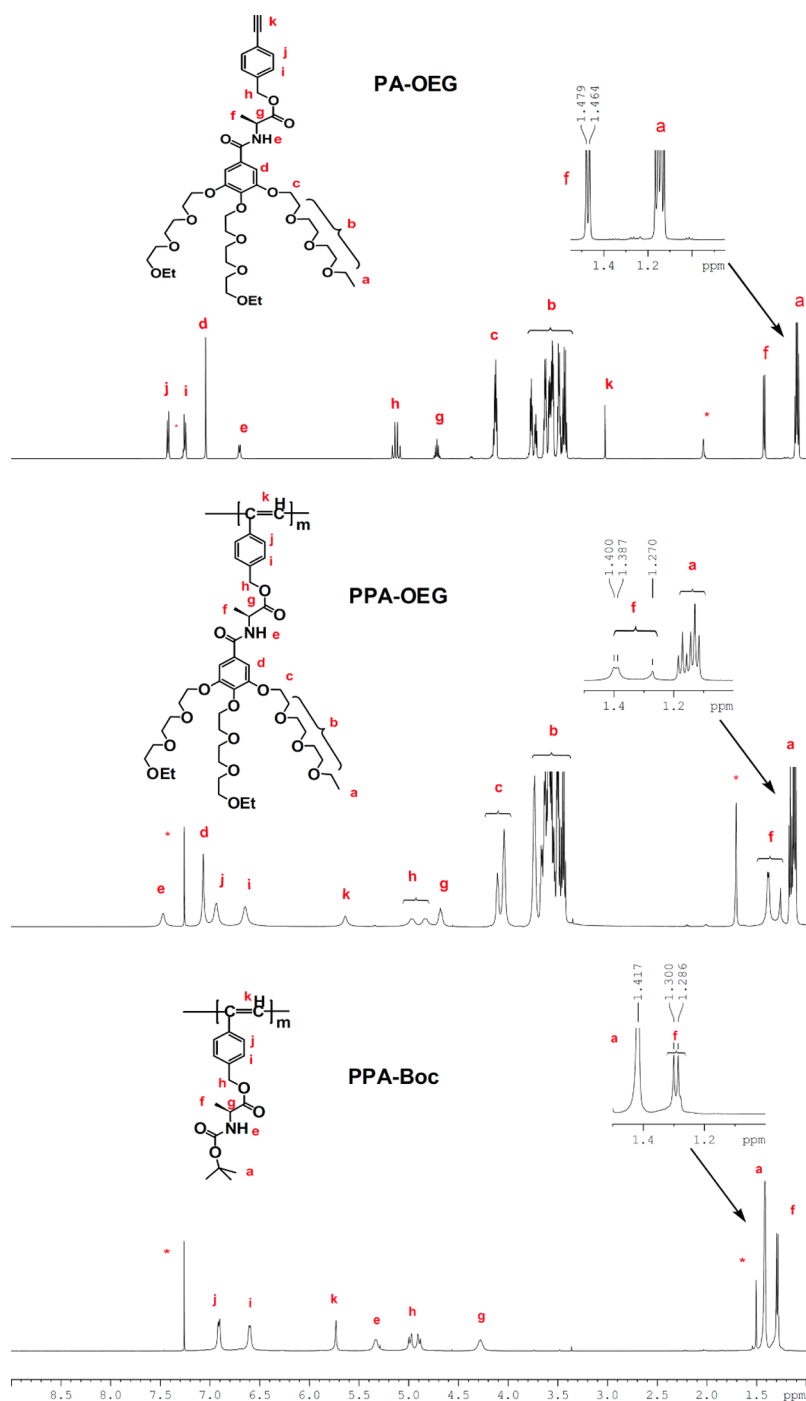


Figure 1. ^1H NMR spectra of monomer PA-OEG (CDCl_3 , 25°C), polymer PPA-OEG (CDCl_3 , 50°C), and polymer PPA-Boc (CDCl_3 , 50°C). The solvent peaks are marked with asterisks.

PPA-OEG, the proton signals (f) split into two asymmetric peaks with intensity ratio around 2:1 at 50°C , and $\Delta\delta$ increased into 0.11 ppm (inset in Figure 1). The asymmetric splitting of proton signals of methyl group from alanine may indicate that PPA-OEG provides a restrained environment, which prevents the methyl group from free rotation. In order to confirm this hypothesis, ^1H NMR spectra of PPA-OEG in $\text{DMSO}-d_6$ were recorded at different temperatures (for spectra, see Figure S1 in the Supporting Information). The proton signals from f split asymmetrically into two peaks at 40, 60, and 80°C . The intensity for the peak at downfield increased with solution temperature, accompanied by diminishing intensity for

the peak at upfield, suggesting that the restrained environment from PPA-OEG mediated the pendants to adopt two possible stable spatial arrangements: one is preferred at low temperature, while the other is favorable at the higher temperature. Similar to its homopolymer PPA-OEG, the copolymer PPA-BDY also showed broad signals in its ^1H NMR spectrum (see Figure S2 in the Supporting Information). Because of the signal broadness, it is difficult to estimate the content of BDY moieties from their ^1H NMR spectra. Instead, the molar contents of BDY units in copolymers were determined by comparison of UV absorbance intensities for the copolymer

with those from the corresponding monomer and were found in the range of 1/1000.

AFM measurements were conducted to directly visualize the morphologies of the helical polymers on substrates. Because of the repulsive effects from bulky dendritic side chain, an extended conformation was expected for these helical polymers, which allows easy visualization of single molecules by AFM. Typical AFM images for PPA-OEG, PPA-BDY, and PPA-Boc are shown in Figure 2. Individual polymer chains can be

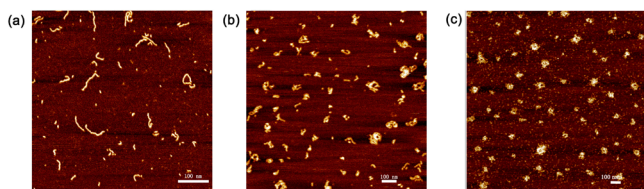


Figure 2. AFM images of (a) PPA-OEG (3.0 mg/L), (b) PPA-BDY (2.6 mg/L), and (c) PPA-Boc (3.2 mg/L) on mica. Samples were prepared from chloroform solutions by spin-coating (2000 rpm). Apparent height ~ 0.5 nm and width ~ 7 nm for PPA-BDY.

identified with length from very short ones to these in the range of a few hundred nanometers for both PPA-OEG and PPA-BDY (Figure 2a,b). In contrast, the model polymer PPA-Boc is much more flexible due to absence of the bulky OEG pendants, and the polymer chains tend to adopt coiled conformation and to aggregate together (Figure 2c).

Thermoresponsive Properties. Except for PPA-Boc, both polymers with rigid poly(phenylacetylene) backbone (PPA-OEG) or flexible polymethacrylate backbone (PMA-OEG) showed good solubility in water at low temperature. Upon heating to elevated temperatures, the slightly yellow but transparent solutions turned opaque due to the thermally induced aggregation of the polymers (see Figure 3a). Therefore, turbidity measurements by using UV/vis spectroscopy were performed to investigate the thermoresponsive behavior of PPA-OEG in detail. Its typical turbidity curves are shown in Figure 3b. Quite fast phase transitions and very small hysteresis were observed. In fact, the two copolymers PPA-BDY and PMA-BDY also show thermoresponsive behavior (for turbidity curves, see Figure S4c,d). T_{cp} s for PPA-OEG, PPA-BDY, and PMA-BDY were determined to be 36.0, 36.2, and 35.0 °C, respectively. These T_{cp} s are very close to one another, suggesting that a trace amount of hydrophobic BDY moiety in the copolymer will not contribute much to the overall hydrophilicity, and both backbone rigidity and helical

conformation do not show obvious influence on the phase transition temperatures.

To further elucidate the thermally induced dehydration processes of these copolymers, temperature-varied ^1H NMR spectroscopy was utilized. The ^1H NMR spectra from PPA-OEG in the temperature range from 24 to 45 °C were assembled in Figure 4. Below its T_{cp} , proton signals ascribed to

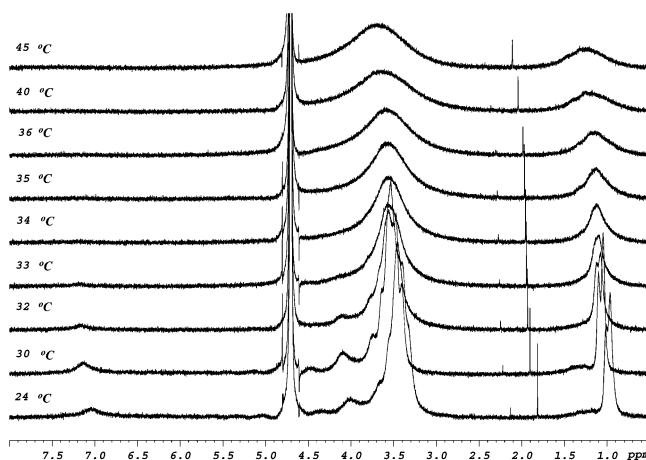


Figure 4. Temperature-varied ^1H NMR spectra of PPA-OEG (0.40 wt %) in D_2O ($T_{cp} = 33.9$ °C).

OEG moieties ($\delta \sim 1.0$ and 3.5 ppm) were quite resolved (the T_{cp} of PPA-OEG determined at this concentration is 33.9 °C; for turbidity curve see Figure S4a). When the temperature rose to 33 °C, which is around its T_{cp} , the proton signals ascribed to OEG dendritic moieties became broader, indicating their dehydration and collapse. The broadening of OEG signals was further enhanced with further temperature increase to above the T_{cp} of PPA-OEG, caused by polymer aggregation. Consistent results were obtained for copolymer PPA-BDY (for ^1H NMR spectra, see Figure S2).

Chiroptical Properties. CD measurements were carried out to investigate whether the chirality could transfer from alanine moieties to the PPA main chain through the ester linkage for PPA-OEG. In addition, its chiroptical properties were monitored during the thermally induced aggregation processes in aqueous solutions to check the possible effects of thermoresponsiveness on the helical conformation. For comparison, chiroptical property of the model polymer PPA-Boc was also examined to check the bulkiness effect from the

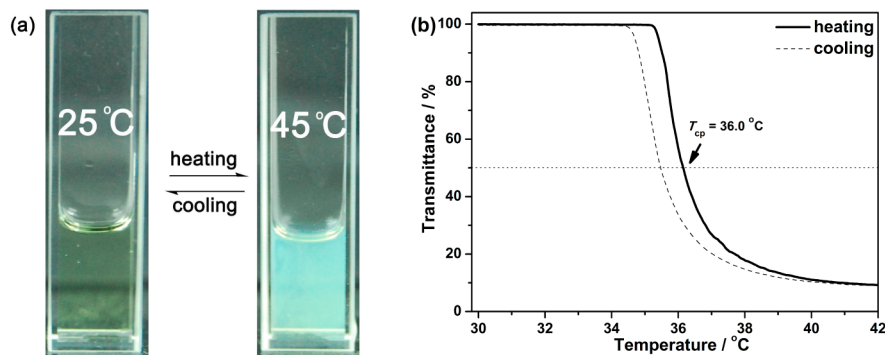


Figure 3. (a) Photographs of PPA-OEG aqueous solutions (0.025 wt %) under visible light at temperature below and above its T_{cp} , respectively. (b) Turbidity curves for PPA-OEG aqueous solution (0.025 wt %). Heating and cooling rate 0.2 K min^{-1} .

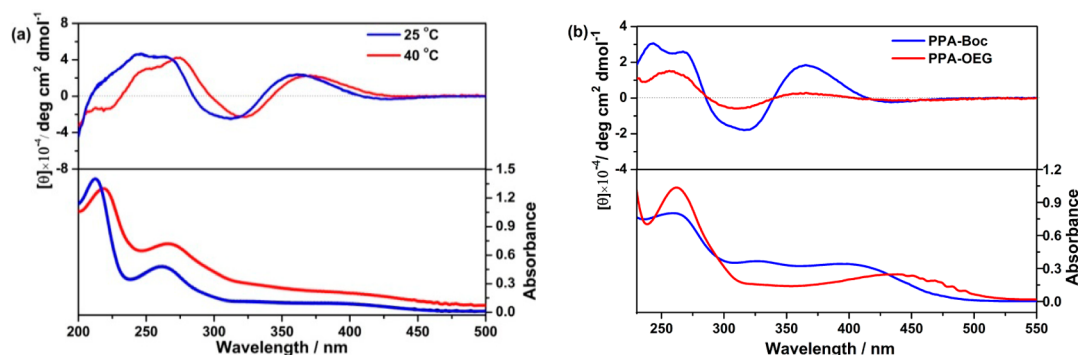


Figure 5. CD and UV/vis spectra for (a) PPA-OEG (0.025 wt %) in aqueous solutions at 25 and 40 °C and (b) PPA-Boc (0.030 wt %) in DCM at 25 °C.

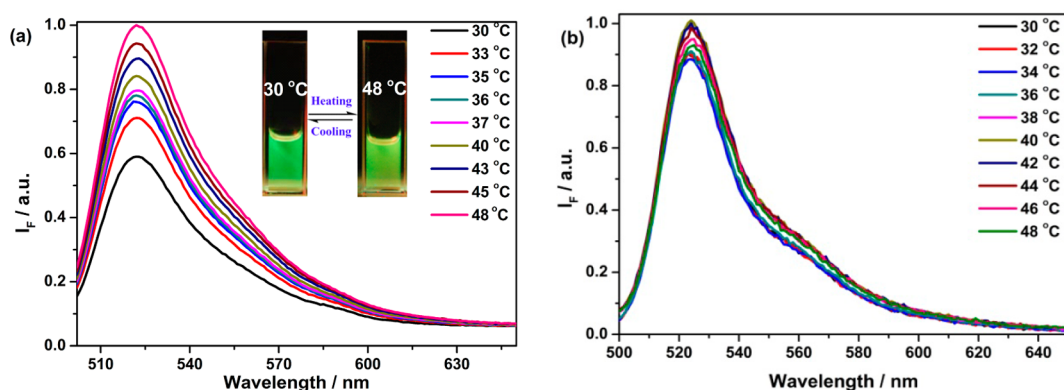


Figure 6. Fluorescence spectra ($\lambda_{\text{ex}} = 490 \text{ nm}$) of aqueous solution of (a) PPA-BDY (0.025 wt %) and (b) PMA-BDY (0.10 wt %) at different temperatures. The fluorescence intensities at their maximum emission ($\lambda_{\text{em}} = 522 \text{ nm}$ for PPA-BDY and $\lambda_{\text{em}} = 524 \text{ nm}$ for PMA-BDY) at 48 °C are set to 1. The inset in (a) shows photographs of aqueous solutions of PPA-BDY (0.025 wt %) under UV irradiation (365 nm) at 30 and 48 °C.

OEG pendants. The CD spectra are shown in Figure 5. From Figure 5a, a strong Cotton effect was observed for PPA-OEG in aqueous solution at 25 °C, indicating that the PPA backbone takes a preferential helical conformation with a large excess in one handedness. Interestingly, after the temperature increased to 40 °C, which is above the phase transition temperature of PPA-OEG ($T_{\text{cp}} = 36.0 \text{ °C}$ at this concentration), the CD spectrum red-shifted more than 10 nm. As the temperature decreased to 25 °C, the original spectrum was almost restored. This red-shift is likely associated with solvophobic collapse of the OEG dendritic pendants.²⁷ In contrast, negligible change was detected in the CD spectrum of PPA-OEG solution in methanol at different temperatures (Figure S5). We believe this red-shift is caused by enhanced steric repulsion from the collapsed OEG dendrons above phase transition temperature, resulting in a stretch of PPA backbone to increase the helical pitch. To the best of our knowledge, this is the first example to report the helical structures of PPAs can be mediated by their thermoresponsiveness in aqueous solutions. However, the Cotton effect of PPA-OEG decreased by about 40% after storage for 3 days (Figure S6), indicating structural isomerization of the PPA main chain as reported previously.²⁸ The model compound PPA-Boc showed even higher molar ellipticity value in DCM than PPA-OEG (Figure 5b), indicating that the bulky OEG dendritic pendant in PPA-OEG is not favorable for the formation of the helical conformation.

Fluorescence Properties. BDY has been proved to be an efficient fluorescent dye which tends to emit relatively sharp fluorescence peaks with high quantum yields, and incorporated

widely in various polymers as dye probe.²⁹ Therefore, helical copolymer PPA-BDY containing a trace amount of BDY chromophore was synthesized and expected to behave as a thermoresponsive fluorescent sensor. As described above, PPA-BDY showed excellent thermoresponsive properties with T_{cp} at 36.2 °C. Thus, fluorescence measurements were performed to monitor its thermoresponsive processes, and the fluorescence spectra are shown in Figure 6a. Significant fluorescence enhancement (Figure S7) was observed when the temperature increased from 30 °C (below T_{cp}) to 48 °C (above T_{cp}). We believe this enhancement is due to confinement environment caused by thermally induced chain collapse and aggregation. At low temperature, the BDY chromophores attached to the rigid backbone through a single bond have the freedom to rotate, which would weaken the fluorescence emission through nonradiative pathway.³⁰ However, when the temperature increased to above T_{cp} , OEG dehydration and collapse, followed by polymer chain aggregation, will provide a confined environment around the BDY chromophores to greatly depress the intramolecular rotation and, in turn, restore the fluorescence intensity. In contrast, the copolymer PMA-BDY with flexible polymethacrylate backbone showed negligible fluorescence enhancement during the thermally induced aggregation processes (temperature from 30 to 48 °C, Figure 6b). UV absorption spectra probably could give some clues for this phenomenon. The aromatic copolymer PPA-BDY and monomer PA-BDY displayed the same absorptions with maximum centered at 500 nm, while aliphatic copolymer PMA-BDY exhibited absorption with maximum centered at 511

nm in DCM, 13 nm red-shifting to that of corresponding aliphatic monomer (Figure S3). This red-shift indicates enhancement of supramolecular interaction between OEG moieties and BDY chromophores within the flexible copolymer. The enhanced interaction might suppress the intramolecular rotation of BDY chromophores even below the phase transition temperature; thus, no obvious fluorescent enhancement was detected during the thermally induced aggregation process. Overall, comparison of fluorescence properties between PPA-BDY and PMA-BDY leads to the conjecture that the supramolecular interactions between OEG moieties and BDY chromophores should be enhanced for the flexible polymers.³¹

CONCLUSIONS

A novel category of poly(phenylacetylene) homo- and copolymers bearing the three-folded oligoethylene glycol dendritic branches were prepared. Their thermoresponsive properties and helical conformation were investigated by UV/vis, CD, and fluorescence spectroscopy. These helical polymers inherited characteristic thermoresponsiveness from their corresponding dendronized polymethacrylate counterparts and showed thermally induced phase transitions with small hysteresis. The L-alanine moiety linked to the main chain through flexible ester linkage could induce the polymers to adopt helical conformation, and this conformation can be reversibly tuned by thermally induced aggregation due to the moderate rigidity of poly(phenylacetylene) backbone. Driven by the thermally induced aggregation, the helical copolymer containing fluorescent BDY chromophores displayed enhanced fluorescence intensity, suggesting that backbone rigidity of the polymer plays an important role. This work is expected to pave a new way for the promising applications of poly(phenylacetylene)s in stimuli-responsive materials and fluorescence probes.

ASSOCIATED CONTENT

Supporting Information

Synthesis and characterization of monomer MA-BDY and polymer PMA-BDY, turbidity curves, as well as additional UV/vis, CD, and NMR spectra. This material is available free of charge via the Internet at <http://pubs.acs.org>.

AUTHOR INFORMATION

Corresponding Authors

*Ph +86-21-66138053; Fax +86-21-66131720; e-mail gckuang@shu.edu.cn (G.K.).

*Ph +86-21-66138053; Fax +86-21-66131720; e-mail azhang@shu.edu.cn (A.Z.).

Notes

The authors declare no competing financial interest.

ACKNOWLEDGMENTS

We thank Dr. Hongmei Deng from the Instrumental Analysis Division of Research Center (Shanghai University) for her assistance in NMR measurements. This work is financially supported by National Natural Science Foundation of China (Nos. 21034004, 21204047, and 21374058) and the Ph.D. Programs Foundation of Ministry of Education of China (No. 201331081100166).

REFERENCES

- (1) Zhu, C. L.; Liu, L. B.; Yang, Q.; Lv, F. T.; Wang, S. *Chem. Rev.* **2012**, *112*, 4687–4735.
- (2) (a) Masuda, T.; Higashimura, T. *Acc. Chem. Res.* **1984**, *17*, 51–56. (b) Aoki, T.; Kaneko, T.; Teraguchi, M. *Polymer* **2006**, *47*, 4867–4892. (c) Liu, J. Z.; Lam, J. W. Y.; Tang, B.-Z. *Chem. Rev.* **2009**, *109*, 5799–5867. (d) Sun, J.-Z.; Qin, A.; Tang, B.-Z. *Polym. Chem.* **2013**, *4*, 211–223.
- (3) (a) Jones, R. A. L. *Nat. Mater.* **2004**, *3*, 209–210. (b) Yashima, E.; Maeda, K.; Lika, H.; Furusho, Y.; Nagai, K. *Chem. Rev.* **2009**, *109*, 6102–6211. (c) Rosen, B. M.; Wilson, C. J.; Wilson, D. A.; Peterca, M.; Imam, M. R.; Percec, V. *Chem. Rev.* **2009**, *109*, 6275–6540. (d) Mao, Y.; Zhang, X.-A.; Xua, H.-P.; Yuan, W.-Z.; Zhao, H.; Qin, A.-J.; Sun, J.-Z.; Tang, B.-Z. *Chin. J. Polym. Sci.* **2011**, *29*, 133–140. (e) Liu, X.; Song, C.; Luo, X.-F.; Yang, W.-T.; Deng, J.-P. *Chin. J. Polym. Sci.* **2013**, *31*, 179–186.
- (4) Nakano, T.; Okamoto, Y. *Chem. Rev.* **2001**, *101*, 4013–4038.
- (5) (a) Lam, J. W. Y.; Kong, X.; Dong, Y.; Cheuk, K. K. L.; Xu, K.; Tang, B.-Z. *Macromolecules* **2000**, *33*, 5027–5040. (b) Cheuk, K. K. L.; Lam, J. W. Y.; Chen, J.; Lai, L.-M.; Tang, B.-Z. *Macromolecules* **2003**, *36*, 5947–5959. (c) Lam, J. W. Y.; Tang, B.-Z. *Acc. Chem. Res.* **2005**, *38*, 745–754.
- (6) (a) Nonokawa, R.; Oobo, M.; Yashima, E. *Macromolecules* **2003**, *36*, 6599–6606. (b) Yashima, E.; Maeda, K.; Nishimura, T. *Chem.—Eur. J.* **2004**, *10*, 42–51. (c) Kamikawa, Y.; Kato, T.; Onouchi, H.; Kashiwagi, D.; Maeda, K.; Yashima, E. *J. Polym. Sci., Part A: Polym. Chem.* **2004**, *42*, 4580–4586.
- (7) (a) Louzao, I.; Seco, J. M.; Quiñoá, E.; Riguera, R. *Angew. Chem., Int. Ed.* **2010**, *49*, 1430–1433. (b) Freire, F.; Seco, J. M.; Quiñoá, E.; Riguera, R. *Angew. Chem., Int. Ed.* **2011**, *50*, 11692–11696.
- (8) (a) Sakurai, S.-i.; Okoshi, K.; Kumaki, J.; Yashima, E. *J. Am. Chem. Soc.* **2006**, *128*, 5650–5651. (b) Leiras, S.; Freire, F.; Seco, J. M.; Quiñoá, E.; Riguera, R. *Chem. Sci.* **2013**, *4*, 2735–2743. (c) Motoshige, R.; Mawatari, Y.; Motoshige, A.; Yoshida, Y.; Sasaki, T.; Yoshimizu, H.; Suzuki, T.; Tsujita, Y.; Tabata, M. *J. Polym. Sci., Part A: Polym. Chem.* **2014**, *52*, 752–759. (d) Fukushima, T.; Takachi, K.; Tsuchihara, K. *Macromolecules* **2008**, *41*, 6659–6601. (e) Fukushima, T.; Kimura, H.; Tsuchihara, K. *Macromolecules* **2009**, *42*, 8619–8626.
- (9) (a) Percec, V.; Rudick, J. G.; Peterca, M.; Heiney, P. A. *J. Am. Chem. Soc.* **2008**, *130*, 7503–7508. (b) Motoshige, A.; Mawatari, Y.; Yoshida, Y.; Motoshige, R.; Tabata, M. *Polym. Chem.* **2014**, *5*, 971–978.
- (10) Maeda, K.; Mochizuki, H.; Osato, K.; Yashima, E. *Macromolecules* **2011**, *44*, 3217–3226.
- (11) Yashima, E.; Maeda, K.; Okamoto, Y. *Nature* **1999**, *399*, 449–451.
- (12) Iida, H.; Mizoguchi, T.; Oh, S.-D.; Yashima, E. *Polym. Chem.* **2010**, *1*, 841–848.
- (13) Zhang, X. A.; Zhao, H.; Cao, Y.; Tong, J.; Shan, L.; Chen, Y.; Zhang, S.; Qin, A.; Sun, J.-Z.; Tang, B.-Z. *Polymer* **2011**, *52*, 5290–5301.
- (14) (a) Kakuchi, R.; Nagata, S.; Sakai, R.; Otsuka, I.; Nakade, H.; Satoh, T.; Kakuchi, T. *Chem.—Eur. J.* **2008**, *14*, 10259–10266. (b) Sakai, R.; Sakai, N.; Satoh, T.; Li, W.; Zhang, A.; Kakuchi, T. *Macromolecules* **2011**, *44*, 4249–4257.
- (15) Sakai, R.; Barasa, E. B.; Sakai, N.; Sato, S.-i.; Satoh, T.; Kakuchi, T. *Macromolecules* **2012**, *45*, 8221–8227.
- (16) Zhang, Y.; Gao, K.; Zhao, Z.; Yue, D.; Hu, Y.; Masuda, T. *J. Polym. Sci., Part A: Polym. Chem.* **2013**, *51*, 5248–5256.
- (17) Hu, G.; Li, W.; Hu, Y.; Xu, A.; Yan, J.; Liu, L.; Zhang, X.; Liu, K.; Zhang, A. *Macromolecules* **2013**, *46*, 1124–1132.
- (18) Kouwer, P. H. J.; Koepf, M.; Le Sage, V. A. A.; Jaspers, M.; van Buul, A. M.; Eksteen-Akeroyd, Z. H.; Woltinge, T.; Schwartz, E.; Kitto, H. J.; Hoogenboom, R.; Picken, S. J.; Nolte, R. J. M.; Mendes, E.; Rowan, A. E. *Nature* **2013**, *493*, 651–655.
- (19) Sakai, N.; Jin, M.; Sato, S.-i.; Satoh, T.; Kakuchi, T. *Polym. Chem.* **2014**, *5*, 1057–1062.
- (20) (a) Li, W.; Zhang, A.; Feldman, K.; Walde, P.; Schlüter, A. D. *Macromolecules* **2008**, *41*, 3659–3667. (b) Li, W.; Zhang, A.; Schlüter,

A. D. *Chem. Commun.* **2008**, 5523–5525. (c) Li, W.; Wu, D. L.; Schlüter, A. D.; Zhang, A. *J. Polym. Sci., Part A: Polym. Chem.* **2009**, *47*, 6630–6640. (d) Junk, M. J. N.; Li, W.; Schlüter, A. D.; Wegner, G.; Spiess, H. W.; Zhang, A.; Hinderberger, D. *Angew. Chem., Int. Ed.* **2010**, *49*, 5683–5687.

(21) (a) Yan, J. T.; Li, W.; Liu, K.; Wu, D. L.; Chen, F.; Wu, P. Y.; Zhang, A. *Chem.—Asian J.* **2011**, *6*, 3260–3269. (b) Yan, J.; Zhang, X.; Li, W.; Zhang, X.; Liu, K.; Wu, P.; Zhang, A. *Soft Matter* **2012**, *8*, 6371–6377.

(22) Benstead, M.; Rosser, G. A.; Beeby, A.; Mehl, G. H.; Boyle, R. W. *Photochem. Photobiol. Sci.* **2011**, *10*, 992–999.

(23) Yuan, W. Z.; Tang, L.; Zhao, H.; Jin, J. K.; Sun, J. Z.; Qin, A. J.; Xu, H. P.; Liu, J. H.; Yang, F.; Zheng, Q.; Chen, E. Q.; Tang, B.-Z. *Macromolecules* **2009**, *42*, 52–61.

(24) Percec, V.; Rudick, J. G.; Peterca, M.; Wagner, M.; Obata, M.; Mitchell, C. M.; Cho, W. D.; Balagurusamy, V. S. K.; Heiney, P. A. *J. Am. Chem. Soc.* **2005**, *127*, 15257–15264.

(25) (a) Hirao, K.; Ishii, Y.; Terao, T.; Kishimoto, Y.; Miyatake, T.; Ikariya, T.; Noyori, R. *Macromolecules* **1998**, *31*, 3405–3408. (b) Kishimoto, Y.; Eckerle, P.; Miyatake, T.; Kainosho, M.; Ono, A.; Ikariya, T.; Noyori, R. *J. Am. Chem. Soc.* **1999**, *121*, 12035–12044.

(26) Simionescu, C. I.; Percec, V.; Dumitrescu, S. *J. Polym. Sci., Polym. Chem. Ed.* **1977**, *15*, 2497–2509.

(27) Percec, V.; Rudick, J. G.; Peterca, M.; Staley, S. R.; Wagner, M.; Obata, M.; Mitchell, C. M.; Cho, W. D.; Balagurusamy, V. S. K.; Lowe, J. N.; Glodde, M.; Weichold, O.; Chung, K. J.; Ghionni, N.; Magonov, S. N.; Heiney, P. A. *Chem.—Eur. J.* **2006**, *12*, 5731–5746.

(28) Percec, V.; Peterca, M.; Rudick, J. G.; Aqad, E.; Imam, M. R.; Heiney, P. A. *Chem.—Eur. J.* **2007**, *13*, 9572–9581.

(29) (a) Loudet, A.; Burgess, K. *Chem. Rev.* **2007**, *107*, 4891–4932. (b) Ulrich, G.; Ziessel, R.; Harriman, A. *Angew. Chem., Int. Ed.* **2008**, *47*, 1184–1201. (c) Boens, N.; Leen, V.; Dehaen, W. *Chem. Soc. Rev.* **2012**, *41*, 1130–1172. (d) Yuan, L.; Lin, W.; Zheng, K.; He, L.; Huang, W. *Chem. Soc. Rev.* **2013**, *42*, 622–661.

(30) Kuimova, M. K.; Yahioglu, G.; Levitt, J. A.; Suhling, K. *J. Am. Chem. Soc.* **2008**, *130*, 6672–6673.

(31) Supramolecular interaction of OEG moieties with dye molecules within dendronized polymers has been revealed in our previous work. See for example: (a) Liu, L. X.; Li, W.; Liu, K.; Yan, J. T.; Hu, G. X.; Zhang, A. *Macromolecules* **2011**, *44*, 8614–8621. (b) Liu, L.; Li, W.; Yan, J.; Zhang, A. *J. Polym. Sci., Part A: Polym. Chem.* **2014**, DOI: 10.1002/pola.27171.